Airy structure in inelastic light-ion and light heavy-ion scattering

F. Michel*
Université de Mons-Hainaut, Place du Parc, 20, B-7000 Mons, Belgium

S. Ohkubo†
Department of Applied Science and Environment, Kochi Women's University, Kochi 780-8515, Japan
(Received 18 December 2003; revised manuscript received 9 July 2004; published 19 October 2004)

We suggest that the transparency displayed by some light heavy-ion systems, such as $^{16}O+^{16}O$, $^{16}O+^{12}C$, or $^{12}C+^{12}C$, which manifests itself by the emergence of Airy structure in the elastic scattering angular distributions and excitation functions, could also have observable consequences in some inelastic channels. Indeed benchmark calculations for the $\alpha+^{40}Ca$ light-ion system, where a similar mechanism dominates elastic scattering at low energy, reveals the persistence in inelastic scattering of the interference mechanism between the barrier-wave and internal-wave components of the scattering amplitude which underlies the Airy structure in the elastic channel. These calculations seem to point to new phase rules between the elastic and inelastic angular distributions.

DOI: 10.1103/PhysRevC.70.044609 PACS number(s): 24.10.Ht, 25.55.Ci, 25.70.Bc

I. INTRODUCTION

Elastic scattering data for some light heavy-ion systems, such as $^{16}O+^{16}O$, $^{16}O+^{12}C$, or $^{12}C+^{12}C$, display distinct refractive features [1]. For example, the 90° excitation functions display gross structure, and/or the angular distributions show a series of broad humps separated by deep minima; at sufficiently high incident energy the differential cross sections decrease exponentially at large angles [2–11].

The refractive features of the data have often been interpreted within a semiclassical framework; for example, the high-energy exponential falloff of the cross sections at large angles is interpreted as a nuclear rainbow, while the deep minima seen in the excitation functions (and in some differential cross sections) are associated with Airy minima. The discussion of these phenomena is generally carried out in terms of the classical concept of deflection function: the nuclear rainbow is associated with the existence of a (negative angle) extremum in the deflection function, and interference between the two branches of the latter accounts for the Airy minima [12].

Optical model (OM) analyses of these data show that they can be described consistently only if the strength of the imaginary part of the optical potential is moderate, in contrast with the situation encountered for most heavy-ion systems where the scattering is governed by strong absorption. An important consequence of this incomplete absorption is that the scattering becomes much more sensitive to the interaction at small internucleus distances, and as a matter of fact this sensitivity has made possible an unambiguous determination of the real part of the potential, well within the strong absorption radius. Contrary to what had been assumed for many years, the real part of the light heavy-ion optical potential is deep; more precisely, its volume integral per nucleon pair $J_v=J_V/A_1A_2$ assumes values of some 350 MeV fm^3 for incident energies of about 10 MeV/nucleon [3,8].

Recently, we have proposed an interpretation of the elastic scattering Airy minima using the so-called barrier-wave–internal-wave (BI) decomposition of the elastic scattering amplitude [13,14]. In this approach, which was originally introduced by Brink and Takigawa within a semiclassical framework [15,16], it is assumed that the effective potential displays an internal pocket for all the active partial waves—which, for the deep potentials discussed here, is guaranteed up to about 10 MeV/nucleon incident energy; the scattering amplitude can then be decomposed into a contribution corresponding to the part of the incident flux which is reflected at the barrier of the effective potential, and a contribution of the part of the flux which passes the potential barrier and reemerges after reflection at the most internal turning point (despite the incomplete absorption multiple reflection remains negligible). We have shown that interference effects between the barrier-wave and internal-wave subamplitudes—which behave smoothly as a function of the angle in the angular region where the Airy minima are observed—account for the Airy structure observed in elastic scattering, and that the two subamplitudes can be associated with each of the branches of the classical deflection function [13,14]. The appearance of Airy minima in the cross section thus requires the existence of a sizeable internal-wave contribution, which in turn confirms in an intuitively obvious way the exceptional transparency of the systems under investigation.

Inelastic or transfer processes have rarely been discussed along these lines; still evidence for the existence of similar phenomena in light heavy-ion nonelastic channels have been presented in the literature. For example, broad structure, similar to that observed in the elastic channel, has been uncovered in the excitation function for the single and mutual excitation of ^{12}C in $^{12}C+^{12}C$ scattering between 30 and 60 MeV center of mass energy, with peak to valley ratios and energy spacings comparable to those seen in the elastic data

*E-mail address: francis.michel@umh.ac.be
†E-mail address: shigeo@cc.kochi-wu.ac.jp

[17]; it has been speculated that this structure could have the same physical origin in the entrance and exit channels [18,19]. The purpose of this paper is to demonstrate that the same interference mechanism can indeed persist in the inelastic scattering angular distributions and excitation functions.

The barrier-wave–internal-wave decomposition has, to the best of our knowledge, never been attempted in nonelastic channels. One probable reason is that the transposition to nonelastic scattering of the semiclassical three-turning point problem is not straightforward. On the other hand for heavy-ion systems systematic measurements in nonelastic channels are scarce; moreover, global optical potentials describing in a precise and detailed way, on broad angular and energy ranges, the elastic *and* inelastic data within the distorted wave Born approximation (DWBA) or coupled channel approaches, are largely lacking.

We therefore decided to test these ideas on a light-ion system which attracted much attention in the past, and for which most of these ingredients are available—that is, $\alpha + {}^{40}$Ca between 24 and 166 MeV; it is also relevant to return to this system since many of the concepts which are currently used to interpret the light heavy-ion data were introduced in earlier studies devoted to this light-ion system [20,21].

II. AIRY STRUCTURE IN ELASTIC AND INELASTIC $\alpha + {}^{40}$Ca SCATTERING

One of the striking features of the $\alpha + {}^{40}$Ca elastic scattering data is the observation of a strong backward rise at large angles, called ALAS (anomalous large angle scattering) because this behavior contrasts with that of many neighboring systems which are conveniently described in terms of strong absorption models. It was shown [20], after many speculations on the mechanism underlying this phenomenon, that—as it proved later to be also the case for the light-heavy ion systems investigated here—this feature is connected with an unusually weak absorption; this incomplete absorption makes possible the emergence of a sizeable internal-wave component, which accounts in a quantitative way for the backward angle behavior at low energy. Moreover, it was shown that a consistent OM description of the energy evolution of the data and, in particular, of the emergence of rainbow scattering at high energy, can only be attained if the real part of the potential is deep (with volume integrals per nucleon pair of about 350 MeV fm^3). Finally, some broad minima observed in the angular distributions at low and intermediate energy could be understood in terms of an interference between the barrier-wave and internal-wave contributions; they thus have the same physical origin as the Airy minima observed in the light heavy-ion systems investigated here. The $\alpha + {}^{40}$Ca elastic scattering data are described in a very satisfactory way between 24 and 166 MeV by the global optical potential of Delbar *et al.* [20], whose parameters vary smoothly and systematically with incident energy.

In addition to numerous precise elastic scattering data, most of which extend on the whole angular range, there exist several interesting inelastic angular distributions for this system. For example, the excitation of several states of ^{40}Ca, including the $J^\pi = 0^+$, $E_x = 3.35$ MeV and $J^\pi = 3^-$, $E_x = 3.73$ MeV states, has been measured on the whole angular range at 29 MeV [22], and angular distributions for excitation of the $J^\pi = 3^-$, $E_x = 3.73$ MeV state, partly presented in Ref. [20], are available in the backward hemisphere for energies ranging from 40 to 62 MeV [23] ; finally one angular distribution for the excitation of the $J^\pi = 0^+$, $E_x = 3.35$ MeV state is also available at 40 MeV in the backward hemisphere [23], and there exists a nearly complete angular distribution for excitation of the $J^\pi = 3^-$ state at $E_\alpha = 100$ MeV [24]. Some of these data have been analyzed successfully in the past within the DWBA approximation [20,25], but they were not subjected to any decomposition, e.g., of the barrier wave–internal-wave type.

Some of these inelastic angular distributions exhibit features which resemble those observed in the elastic channel: for example, at 29 MeV incident energy, the angular distribution for excitation of the $J^\pi = 0^+$, $E_x = 3.35$ MeV state displays a backward enhancement very similar to that seen in the elastic data, and around 45 MeV incident energy the backward angular distributions for the excitation of the $J^\pi = 3^-$, $E_x = 3.73$ MeV state present a minimum at an angle not far from an Airy minimum seen in the elastic angular distributions at the same energies. And at $E_\alpha = 100$ MeV, both the elastic and the $J^\pi = 3^-$ inelastic angular distributions display an exponentially decreasing behavior at large angles, with comparable slopes.

In the elastic channel, it is possible to circumvent the difficult semiclassical calculations (location of complex turning points, calculation of several action integrals in the complex plane) needed to isolate the barrier-wave and internal-wave contributions to the scattering amplitude [15,16]; indeed it has been shown [26] that the relevant information can be obtained in a reliable way by performing several conventional OM calculations with modified versions of the original optical potential. For example, the BI decomposition can be carried out by analyzing the response of the elastic S matrix to perturbations of the potential in the internal region [26]. More simply, the barrier component of the scattering amplitude can be obtained by enhancing significantly the absorption in the internal region, which has the effect to suppress the internal contribution; the latter can then be extracted by subtracting the barrier contribution from the full scattering amplitude.

The second method must be used with some caution, however, because the strong and short-ranged extra absorption needed to suppress the internal component can in some cases produce unwanted spurious reflection; the quality of the results obtained can, however, be checked relatively easily: different parametrizations of the additional absorptive term should lead to nearly identical results. More directly, one can check the validity of the calculations in the elastic channel against full semiclassical calculations. Because of its simplicity this method can hopefully be extended to the inelastic channels; this should especially be the case for calculations carried out within the DWBA approximation: indeed one expects that calculations carried out with distorted waves obtained by using this extra absorption should provide the barrier contribution to the inelastic transition matrix, and

thus to the inelastic scattering amplitude; again a simple subtraction should in a second step provide the internal contribution to these quantities.

In the case of the $\alpha+^{40}$Ca system, we first applied this scheme to the excitation of the $J^\pi=0^+$, $E_x=3.35$ MeV state at 29 and 40 MeV incident energies. At 29 MeV, the global optical potential of Delbar *et al.* [20] correctly describes the main trends of the elastic scattering data [27], but a fine-tuning of the real and imaginary wells parameters results in a more quantitative agreement (for example, the 29 MeV data are better described when the parameters of the Woods-Saxon squared real and imaginary parts of the Delbar potential are tuned to the values $U_0=190.2$ MeV, $R=4.622$ fm, $a=0.645$ fm, and $W_0=19.4$ MeV, $R_W=5.025$ fm, and $a_W=0.649$ fm; with a volume integral per nucleon pair of 356.0 MeV fm^3, this potential is close to the original Delbar potential—the volume integral of the latter at 29 MeV is 365.2 MeV fm^3). At 40 MeV the optical potential used in the calculations is the global potential of Delbar *et al.* [20].

Here and in the following, use was made of the coupled channel code ECIS [28] and of a standard vibrational (real) collective form factor. Such a form factor is *a priori* inappropriate for describing the transition to the $J^\pi=0^+$, $E_x=3.35$ MeV state—as would also be the popular volume + surface term used to describe, e.g., the excitation of the giant monopole resonance [29]. Indeed this state is known to be a $4p$-$4h$ deformed state, with an $\alpha+^{36}$Ar cluster structure, on which is built a $K^\pi=0^+$ rotational band, comprising the $J^\pi=2^+$, $E_x=3.90$ MeV and $J^\pi=4^+$, $E_x=5.28$ MeV states. An adequate coupling form factor should thus, in principle, be derived from some microscopic approach; this lies clearly outside the scope of this work. However, as one of the main results of the present study is to reveal a sensitivity of the inelastic $\alpha+^{40}$Ca cross sections to the interaction at small distances, similar to that found in the elastic channel, the $\alpha+^{40}$Ca system provides a unique opportunity to compare the merits of the inelastic coupling form factors supplied by various microscopic models on a broad radial range. We would like to note that, because we describe elastic scattering using a Woods-Saxon squared potential—which has a shape closely approximating that of the folding model potentials—the vibrational form factor used here is not so sharply located at the nuclear surface as those derived from conventional Woods-Saxon potentials. This is illustrated in Fig. 1, where the inelastic form factor of the present calculation is compared with that derived from the Woods-Saxon potential of Gaul *et al.* [30], a potential which is unable to reproduce ALAS but describes satisfactorily elastic α-particle scattering from "normal" targets in the $A=40$ mass region.

As can be seen in Fig. 2, the use of the inelastic vibrational form factor derived from the Woods-Saxon squared potential leads to quite a reasonable agreement with the limited set of data investigated here; the "phonon amplitude" β_0 (which is nothing here but a scaling factor) assumes the same value (0.017) at the two energies. In particular the calculations reproduce the characteristic behavior of the back angle data nicely, which is very similar to that observed in the elastic channel (the oscillations in both channels are nearly in phase at each energy).

One remarkable feature of the calculated inelastic cross section is the appearance of deep minima, similar to those

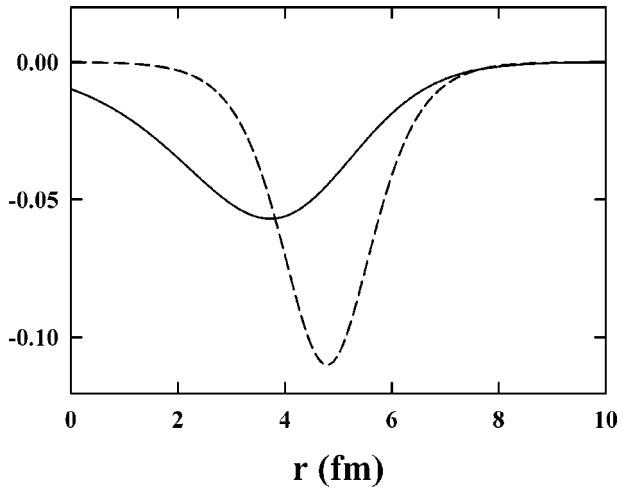

FIG. 1. Comparison of the inelastic form factor (arbitrary units) used in this work to describe the excitation of the $J^\pi=0^+, E_x=3.35$ MeV state (full line), with the vibrational form factor derived from the Woods-Saxon potential of Gaul *et al.* [30] (dashed line).

seen in the elastic channel. This is particularly clear at 40 MeV, where two such minima are predicted around $\Theta_{\text{c.m.}}=45°$ and 90°. Unfortunately no measurements are available at 40 MeV in the relevant angular region to ascertain the existence of these minima; the second minimum is close to that observed in the elastic channel at about 85°. At 29 MeV the broad minimum predicted by the calculation around $\Theta_{\text{c.m.}}=75°$ falls not far from the experimental sharp minimum near $\Theta_{\text{c.m.}}=85°$.

We next attempted to extract the barrier-wave component from the elastic and inelastic scattering amplitudes by introducing, as explained above, a strong additional absorption in the region of the potential pocket corresponding to the grazing angular momentum. This was performed conveniently in the code ECIS by introducing an additional absorptive term of the "surface" type, but much stronger and peaking at a much smaller distance than those used to describe surface absorption; as an indication, the parameters of the Woods-Saxon derivative term used for that purpose at 40 MeV are, in conventional notations, $W_s=50$ MeV, $R_s=3.75$ fm, and $a_s=0.50$ fm. The results obtained in the elastic channel do not depend critically on the parameters used, and they are very close to those given by a semiclassical code; we therefore have every reason to believe that the results obtained in the inelastic channel are reliable too. The internal-wave contribution to the scattering was obtained in a second step, by subtracting the barrier-wave contribution from the total scattering amplitude; the corresponding cross sections are also displayed in Fig. 2.

As in the elastic channel, it is seen that the barrier-wave contribution dominates inelastic scattering at small angles, while the internal-wave component explains the oscillations of the back angle data; and as in the elastic case, both contributions are essentially smooth in the region of the deep minima, which thus originate from an interference mechanism between these two subamplitudes: in other words the deep minima seen in the inelastic channel have exactly the same physical origin as in the elastic channel, and can thus rightly be termed "inelastic Airy minima."

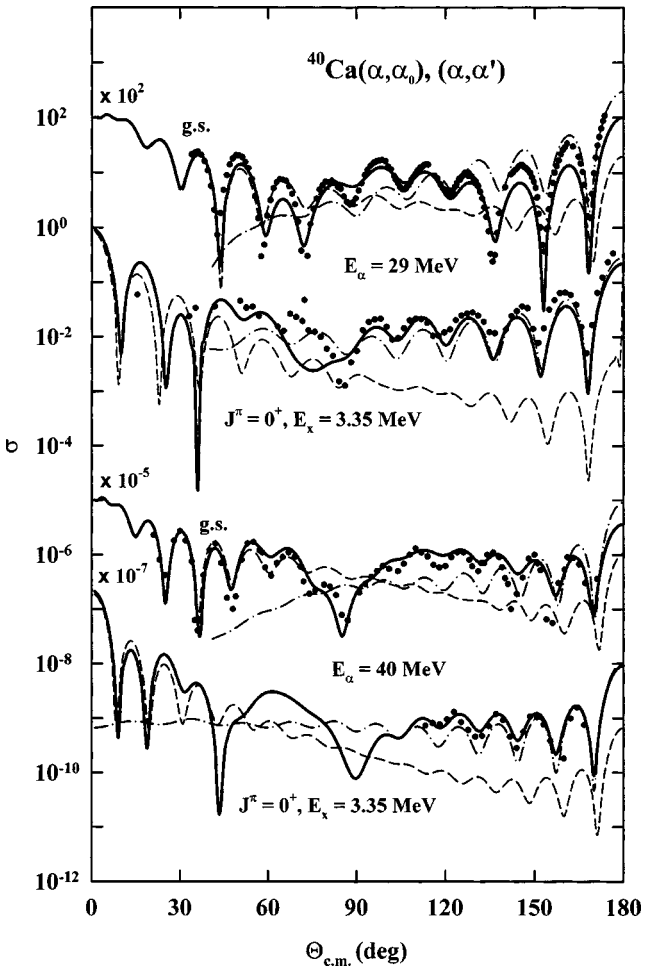

FIG. 2. Barrier-wave–internal-wave contributions to the elastic and inelastic ($J^\pi=0^+, E_x=3.35$ MeV)$\alpha+^{40}$Ca angular distributions at 29 and 40 MeV incident energies (thick line: full cross section, dashed line: barrier-wave contribution, dash-dotted line: internal-wave contribution; in all the figures, the elastic cross sections are given as ratios to Rutherford, inelastic cross sections in mb/sr). The 29 MeV elastic data, the 29 MeV inelastic data and the 40 MeV data are taken from Refs. [27], [22], and [20,23], respectively.

It is also interesting to compare the behavior of the elastic and inelastic S matrices corresponding to the different contributions to the elastic and inelastic scattering amplitudes. A look at Fig. 3 shows that, as in the elastic channel, the inelastic barrier-wave and internal-wave S matrices have very little overlap in angular momentum space; moreover the localization in ℓ space of the two components is seen to be similar in both channels.

We next investigated in the same spirit the excitation of the $J^\pi=3^-$, $E_x=3.73$ MeV vibrational state, for which several complete experimental angular distributions, and many angular distributions in the backward hemisphere, are available. The calculations were again carried out within the frame of the DWBA, using the global optical potential of Delbar *et al.*; all the calculations presented correspond to the energy-independent value $\beta_3=0.22$ for the coupling parameter, which is in good agreement with values extracted from other reactions (see Ref. [20], and references therein). As can be

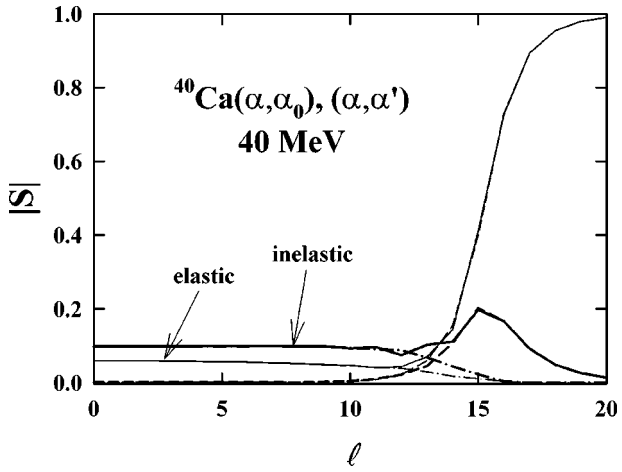

FIG. 3. Barrier-wave–internal-wave contributions to the modulus of the $\alpha+^{40}$Ca elastic and inelastic ($J^\pi=0^+, E_x=3.35$ MeV) S matrix at 40 MeV incident energy (thin lines: elastic, thick lines: inelastic, full lines: full S matrix, dashed line: barrier-wave contribution, dash-dotted line: internal-wave contribution).

seen in Fig. 4, where the optical model elastic scattering angular distributions at the same energies are also displayed, the calculations reproduce nicely the data on the whole energy range. In particular the characteristic evolution with en-

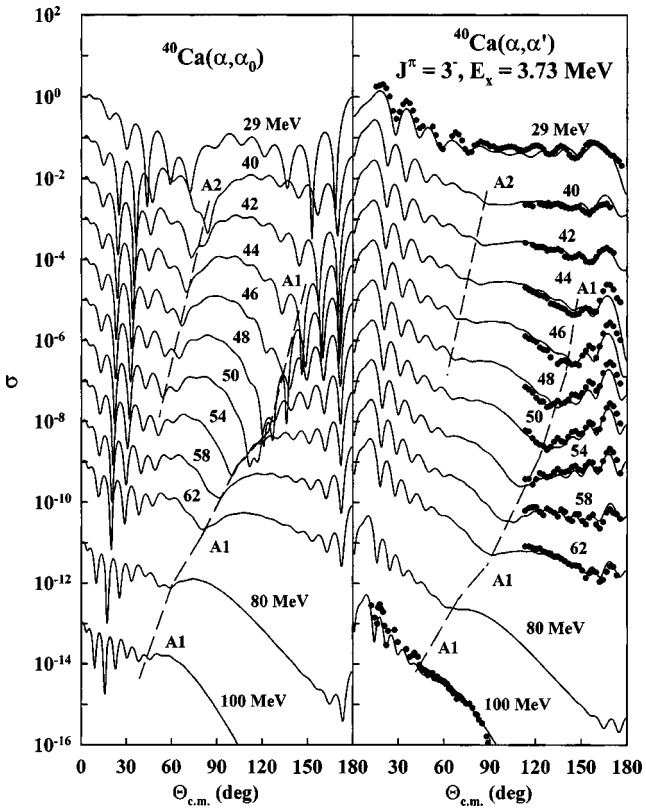

FIG. 4. Elastic (left) and inelastic ($J^\pi=3^-, E_x=3.73$ MeV, right) $\alpha+^{40}$Ca angular distributions between 28 and 100 MeV, showing the evolution with energy of the position of the A1 and A2 Airy minima; each successive angular distribution is shifted downwards by one or two decades (data at 29 MeV, from 40 to 62 MeV, and at 100 MeV from Refs. [22], [20,23], and [24], respectively).

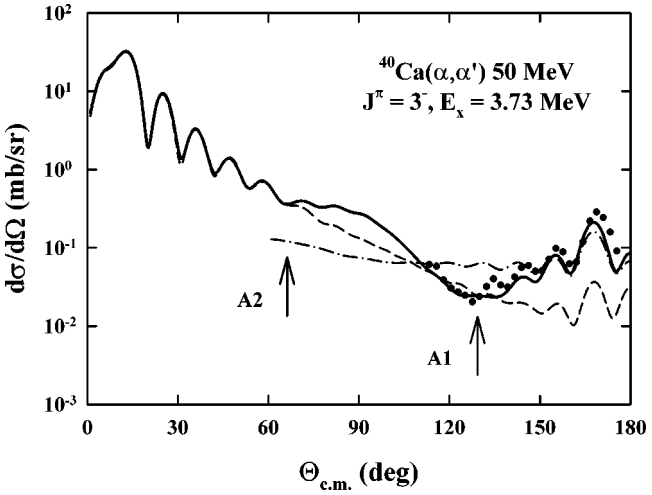

FIG. 5. Barrier-wave–internal-wave contributions to the $\alpha + ^{40}$Ca inelastic angular distribution for excitation of the $J^\pi = 3^-, E_x = 3.73$ MeV state at 40 MeV incident energy (thick line: full cross section, dashed line: barrier-wave contribution, dash-dotted line: internal-wave contribution); the arrows point to the two inelastic Airy minima, which are seen to result from an interference between the barrier-wave and internal-wave contributions to the inelastic scattering amplitude.

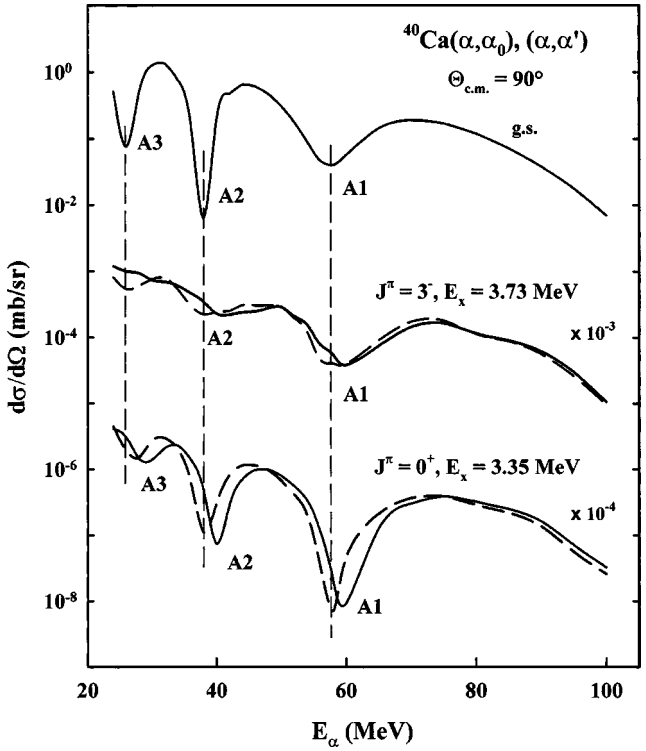

FIG. 6. Elastic and inelastic $\alpha + ^{40}$Ca excitation functions at 90°; for the inelastic excitation functions, the dashed lines give the result of DWBA calculations carried out within the adiabatic approximation ($E_x = 0$).

ergy of the backward rise of the data is well accounted for.

Most noticeable in this context is the presence in the inelastic angular distributions of two minima whose position changes with incident energy; whereas the minimum at smaller angles cannot be seen in the incomplete available experimental data, the second one is clearly seen experimentally from 44 to 50 MeV. A barrier-wave–internal-wave decomposition of the inelastic scattering amplitude, similar to that performed for the $J^\pi = 0^+$, $E_x = 3.35$ MeV state, reveals again that, although several matrix elements now contribute to the scattering for each angular momentum, interference effects between the two subamplitudes are still responsible for these broad dips; this decomposition is presented for $E_\alpha = 50$ MeV in Fig. 5, which demonstrates clearly how the presence of an internal component is crucial to create the observed Airy pattern. Figure 4 revealed the close parallel in the energy behavior of these interference phenomena in the elastic and inelastic channels: this allows us to identify the inelastic minima with the same labels as in the elastic channel. At high energy, where a BI decomposition is no more feasible because of the disappearance of the pocket in the effective potential curves near the grazing angular momentum, the elastic *and* inelastic angular distributions turn to a characteristic rainbow pattern.

The strong correlation between the elastic and inelastic Airy minima is still better displayed in Fig. 6, where we present excitation functions at 90° for the three channels investigated here. Beyond the similarity between the three curves, the most noticeable feature here is the systematic shift towards higher energy of the Airy minima in the inelastic excitation functions. It can be seen that this shift is connected with the finite excitation energy of these states: indeed repeating the same calculations within the adiabatic approximation ($E_x = 0$) now locates the inelastic minimum at virtually the same energy as in the elastic channel (Fig. 6). It is interesting to point out that such a correlation was remarked long ago by Marty [18], and recently emphasized by Nicoli *et al.* [19] in the case of the $^{12}C + ^{12}C$ system; indeed these authors speculated that the minima seen in the inelastic channels corresponding to the single and to the mutual excitation of ^{12}C to its $J^\pi = 2^+$, $E_x = 4.43$ MeV rotational state could be ghosts of those seen in the elastic channel, but shifted towards the *lower* energies by once or twice the excitation energy of ^{12}C; the results reported here point to a similar result, except that the sign of the shift found is opposite to that reported in Refs. [18] and [19]. The explanation of the energy shift reported here seems rather natural: indeed after an inelastic transition, the system has *lost* kinetic energy, and it requires a higher incident energy to recover the same kinematical conditions.

III. AIRY STRUCTURE IN INELASTIC LIGHT HEAVY-ION SCATTERING

We finally return briefly to the case of light heavy-ion scattering. Since Airy minima, connected to the exceptional transparency of some systems, have clearly been observed experimentally, and since the interference mechanism which is responsible for their appearance does, as is supported by the present calculations, survive in some inelastic channels, we believe that such a mechanism has a chance to be also observed in several light heavy-ion systems. In Fig. 7, we present tentative calculations, performed for the $^{16}O + ^{16}O$

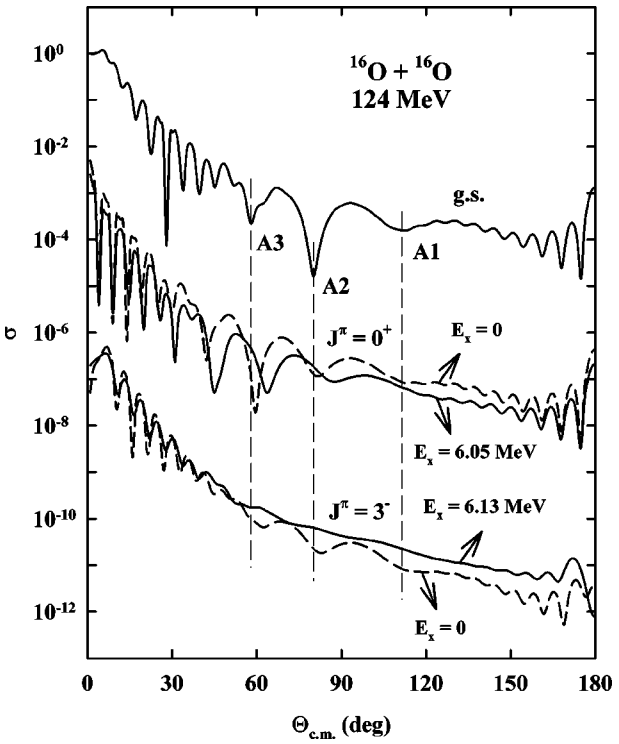

FIG. 7. Nonsymmetrized elastic and inelastic $^{16}O+^{16}O$ angular distributions at 124 MeV calculated using the potential of Nicoli [31] ; the inelastic cross sections for excitation of the $J^\pi=0^+, E_x=6.05$ MeV and $J^\pi=3^-, E_x=6.13$ MeV states were also calculated within the adiabatic approximation (dashed lines).

system at 124 MeV, using the optical potential of Nicoli *et al.* [31], and using the DWBA approximation to describe the transition to the first two excited states in ^{16}O, which are physically similar to those we considered in the $\alpha+^{40}Ca$ case: the $4p-4h$, $J^\pi=0^+$, $E_x=6.05$ MeV $\alpha+^{12}C$ cluster state, and the $J^\pi=3^-$, $E_x=6.13$ MeV vibrational state; as no experimental data are available in this case, the calculations were performed using an arbitrary phonon amplitude, and the inelastic cross sections of Fig. 7 are thus presented in arbitrary units.

The calculations were repeated in the adiabatic approximation ($E_x=0$) to investigate further the role of the excitation energy in the building up of the inelastic Airy minima; these calculations confirm our earlier findings, that is, the appearance of Airy minima similar to those seen in the elastic angular distribution, but shifted towards larger angles when the excitation energy of the state is taken into account. Some higher order Airy minima, which are not seen in the elastic angular distribution at small angles, are even more apparent in the inelastic channel; note, however, that the angular distributions presented here have not been symmetrized, and that minima far from $\Theta=90°$ are not expected to be easily detected in experimental angular distributions. In the case of the $J^\pi=3^-$, $E_x=6.13$ MeV state, the situation seems to be less favorable: indeed if Airy minima are clearly apparent in the calculation carried out with $E_x=0$, they tend to be washed out when use is made of the physical excitation energy. An additional problem is that these two states are nearly degenerate and thus difficult to disentangle experimentally; however, evidence for the predicted Airy minima could possibly persist in the incoherent sum of the two cross sections, and thus show up in the unresolved angular distributions or excitation function for the two states.

IV. CONCLUSIONS

In conclusion, the calculations reported here suggest that the transparency seen in some light heavy-ion systems—which manifests itself in the form of Airy structure in the elastic scattering data—could have observable consequences in some inelastic channels as well: a very comparable mechanism, that is, an interference between barrier-wave and internal-wave components of the inelastic scattering amplitude, should produce a similar structure, with a shift in energy comparable to the energy of the state excited.

In the adiabatic approximation, the elastic and inelastic Airy minima observed at intermediate angles are found to be located at closely similar angles, which suggests the existence of a kind of new "phase rule;" preliminary calculations indicate that the latter does not seem to depend on the spin of the state excited. The same calculations also indicate that the minima of the inelastic internal-wave contribution at large angles are in phase with those seen in the elastic channel, whatever the spin of the excited state—another phase rule which contrasts with the familiar Blair phase rule observed at small angles in the context of strong absorption [29]. These interesting effects will be investigated further in a forthcoming publication.

The transparency implied by the existence of a sizeable internal contribution to inelastic scattering opens the possibility to investigate, when more comprehensive data become available, the shape of the inelastic coupling form factor in more detail—not only for the nonstandard $L=0$ and $L=1$ monopole and dipole cases, but also for higher multipolarities, as suggested by the recent work of Khoa and Satchler, where the limits of the use of the conventional deformed potential were pointed out [32]. Whereas this structure has possibly already been observed in the single or mutual excitation of ^{12}C in $^{12}C+^{12}C$ scattering, it could also manifest itself in systems such as $^{16}O+^{16}O$ or $^{16}O+^{12}C$, or even in a system such as $^{16}O+^{40}Ca$, which has not been thoroughly investigated at the energies and angles of interest but also seems to be a promising candidate.

ACKNOWLEDGMENTS

One of the authors (S.O.) thanks Professor M. S. Hussein and Professor D. T. Khoa for valuable discussions.

[1] M. E. Brandan and G. R. Satchler, Phys. Rep. **285**, 143 (1997), and references therein.
[2] A. A. Ogloblin, Dao T. Khoa, Y. Kondō, Yu. A. Glukhov, A. S. Dem'yanova, M. V. Rozhkov, G. R. Satchler, and S. A. Goncharov, Phys. Rev. C **57**, 1797 (1998).
[3] M. P. Nicoli, F. Haas, R. M. Freeman, S. Szilner, Z. Basrak, A. Morsad, G. R. Satchler, and M. E. Brandan, Phys. Rev. C **61**, 034609 (2000).
[4] A. A. Ogloblin, Yu. A. Glukhov, W. H. Trzaska, A. S. Dem'yanova, S. A. Goncharov, R. Julin, S. V. Klebnikov, M. Mutterer, M. V. Rozhkov, V. P. Rudakov, G. P. Tiorin, Dao T. Khoa, and G. R. Satchler, Phys. Rev. C **62**, 044601 (2000).
[5] M. E. Brandan, A. Menchaca-Rocha, L. Trache, H. L. Clark, A. Ahzari, C. A. Gagliardi, Y.-W. Lui, R. E. Tribble, R. L. Varner, J. R. Beene, and G. R. Satchler, Nucl. Phys. **A688**, 659 (2001).
[6] S. Szilner, M. P. Nicoli, Z. Basrak, R. M. Freeman, F. Haas, A. Morsad, M. E. Brandan, and G. R. Satchler, Phys. Rev. C **64**, 064614 (2001).
[7] Y. Kondō, Y. Sugiyama, Y. Tomita, Y. Yamanouchi, H. Ikezoe, K. Ideno, S. Hamada, T. Sugimitsu, M. Hijiya, and H. Fujita, Phys. Lett. B **365**, 17 (1996).
[8] M. P. Nicoli, F. Haas, R. M. Freeman, N. Aissaoui, C. Beck, A. Elanique, R. Nouicer, A. Morsad, S. Szilner, Z. Basrak, M. E. Brandan, and G. R. Satchler, Phys. Rev. C **60**, 064608 (1999).
[9] Dao T. Khoa, W. von Oertzen, H. G. Bohlen, and F. Nuoffer, Nucl. Phys. **A672**, 387 (2000).
[10] H. G. Bohlen, X. S. Chen, J. G. Kramer, P. Fröbrich, B. Gebauer, H. Lettau, A. Miczaika, W. von Oertzen, R. Ulrich, and T. Wilpert, Z. Phys. A **322**, 241 (1985).
[11] M. E. Brandan, M. Rodríguez-Villafuerte, and A. Ayala, Phys. Rev. C **41**, 1520 (1990).
[12] M. S. Hussein and K. W. McVoy, Prog. Part. Nucl. Phys. **12**, 103 (1984).
[13] F. Michel, F. Brau, G. Reidemeister, and S. Ohkubo, Phys. Rev. Lett. **85**, 1823 (2000).
[14] F. Michel, G. Reidemeister, and S. Ohkubo, Phys. Rev. C **63**, 034620 (2001).
[15] D. M. Brink and N. Takigawa, Nucl. Phys. **A279**, 159 (1977).
[16] D. M. Brink, *Semi-classical Methods for Nucleus-Nucleus Scattering* (Cambridge University Press, Cambridge, 1985).
[17] A. Morsad, F. Haas, C. Beck, and R. M. Freeman, Z. Phys. A **338**, 61 (1991).
[18] C. Marty, *Proceedings of the Symposium on Heavy-ion Elastic Scattering*, Rochester, 1977, edited by R. M. DeVries, p. 507.
[19] M. P. Nicoli, S. Szilner, F. Haas, R. M. Freeman, N. Aissaoui, C. Beck, A. Elanique, R. Nouicer, A. Morsad, Z. Basrak, M. E. Brandan, G. R. Satchler, and Charissa Collaboration, *Proceedings 7th International Conference on Clustering Aspects of Nuclear Structure and Dynamics*, Rab, Croatia, 1999, edited by M. Korolija, Z. Basrak, and R. Kaplar (World Scientific, Singapore, 2000), p. 151.
[20] Th. Delbar, Gh. Grégoire, G. Paić, R. Ceuleneer, F. Michel, R. Vanderpoorten, A. Budzanowski, H. Dabrowski, L. Freindl, K. Grotowski, S. Micek, R. Płaneta, A. Strzalkowski, and K. A. Eberhard, Phys. Rev. C **18**, 1237 (1978).
[21] see, e.g., F. Michel, S. Ohkubo, and G. Reidemeister, Prog. Theor. Phys. Suppl. **132**, 7 (1998), and references therein.
[22] N. Schmeing and R. Santo, Phys. Lett. **33B**, 219 (1970).
[23] Th. Delbar (private communication).
[24] H. Eickhoff, D. Frekers, H. Löhner, K. Poppensieker, R. Santo, G. Gaul, C. Mayer-Böricke, and P. Turek, Nucl. Phys. **A252**, 333 (1975).
[25] A. M. Kobos, B. A. Brown, R. Lindsay, and G. R. Satchler, Nucl. Phys. **A425**, 205 (1984).
[26] J. Albiński and F. Michel, Phys. Rev. C **25**, 213 (1982).
[27] H. P. Gubler, U. Kiebele, H. O. Meyer, G. R. Plattner, and I. Sick, Nucl. Phys. **A351**, 29 (1981).
[28] J. Raynal, *Proceedings of the International Conference on Computing as a Language of Physics*, ICTP, Trieste, 1971 (IAEA, Vienna, 1972), p. 281.
[29] G. R. Satchler, *Direct Nuclear Reactions* (Clarendon Press, Oxford, 1983).
[30] G. Gaul, H. Lüdecke, R. Santo, H. Schmeing, and R. Stock, Nucl. Phys. **A137**, 177 (1969).
[31] M. P. Nicoli, Ph.D. thesis, Strasbourg, 1998.
[32] Dao T. Khoa and G. R. Satchler, Nucl. Phys. **A668**, 3 (2000).